RIGA TECHNICAL UNIVERSITY

Rolands SAVELIS

STUDY OF SIGNAL SAMPLING AND RECONSTRUCTION METHODS

Summary of Doctoral Thesis

The doctoral thesis was carried out at the Institute of Electronics and Computer Science

Riga 2013

RIGA TECHNICAL UNIVERSITY
Faculty of Electronics and Telecommunications
Institute of Radio Electronics

Rolands SAVELIS
Doctoral program "Electronics"

STUDY OF SIGNAL SAMPLING AND RECONSTRUCTION METHODS

Summary of Doctoral Thesis

The doctoral thesis was carried out at the Institute of Electronics and Computer Science

Supervisor
Dr.sc.comp., senior researcher
M.GREITANS

Riga 2013

UDK 621.391 (043.2)
Šā 920 s

Savelis R. Study of signal sampling and reconstruction methods. Summary of the doctoral thesis.-R.:RTU, 2013.-36 p.

Printed according to the decision of the Doctoral Committee “RTU P-08”, June 27, 2013, Protocol No. 16.

This work has been supported by the European Social Fund within the project “Support for the implementation of doctoral studies at Riga Technical University”.

This work is the result of the research carried out at the Institute of Electronics and Computer Science within the framework of the State research program “Scientific basis of information technologies” project No.3 “Research and development of original signal processing approaches for creation of competitive IT technologies” and ESF co-financed project No.2009/0219/1DP/1.1.1.2.0/APIA/VIAA/020 “R&D Center for Smart Sensors and Networked Embedded Systems”.

ISBN ...

**DOCTORAL THESIS
SUBMITTED FOR THE DEGREE OF DOCTOR OF ENGINEERING SCIENCES AT RIGA TECHNICAL UNIVERSITY**

The doctoral thesis for the degree of Doctor of engineering sciences will be defended on October 31, 2013 at 17:45 at Institute of Electronics and Computer Science, 14 Dzerbenes street, auditorium 101B.

OFFICIAL REVIEWERS

Dr.sc.ing., Prof. Peteris Misans
Faculty of Electronics and Telecommunications, Riga Technical University

Dr.phys. Janis Trokss
Faculty of Information Technologies, Ventspils University College

Dr.math. Maris Alberts
Institute of Mathematics and Computer Science, University of Latvia

CONFIRMATION

I confirm that I have developed this thesis, which is submitted for the degree of Doctor of engineering sciences at Riga Technical University. This thesis has not been submitted for the degree of Doctor at an other university.

Rolands Savelis ……………………………. (Signiture)

Date: ………………………

The doctoral thesis is written in Latvian, contains introduction, five chapters, conclusions, references, 8 appendices, 61 figures, 132 pages in total. A list of references consists of 108 sources.

CONTENTS

Abbreviations

ADC	Analog-to-digital converter
AADC	Asynchronous analog-to-digital converter
DAC	Digital-to-analog converter
CS	Compressive sensing
DASP	Digital alias-free signal processing
DFT	Discrete Fourier transform
EFS	Extended Fourier series
EFT	Extended Fourier transform
EMD	Empirical Mode Decomposition
FROI	Finite rate of innovation
FS	Fourier series
FT	Fourier transform
IEFT	Inverse extended Fourier transform
LC	Level-crossing
STFT	Short-time Fourier transform

Symbols and notations

Symbol	Interpretation
f	Frequency
f_d	Sampling frequency
$f_{max}(t)$	Maximum instantaneous frequency
F_{max}	Maximum frequency
$F[s(t)]$	Fourier transform
$F^{-1}[S(\omega)]$	Inverse Fourier transform
$\tilde{F}[s(t), g(t)]$	Extended Fourier transform
$\tilde{F}^{-1}[S(\omega_g), g(t)]$	Extended inverse Fourier transform
$h(t)$	Impulse response
L_2	Hilbert space
$s(n)$	Discrete signal
$s(t)$	Continuous time signal
$\hat{s}(t)$	Approximation
$s'(t)$	Derivative
$s^{(-1)}(\cdot)$	Inverse of the signal
$S(f)$, $S(\omega)$	Spectrum obtained by Fourier transform
$S(\omega_g)$	Spectrum obtained by Extended Fourier transform
$S(t, f)$	Time-frequency distribution
t, τ	Continuous time
t_n	Discrete time
T	Sampling step
$V(\varphi)$	Approximation space
Z	Set of integers
$\delta(t)$	Dirac delta function
Δl	Distance between uniformly distributed levels
Δt_n	Distance between consecutive samples
Δt_{max}	Maximum distance consecutive samples
Θ	Signal period/duration
Υ	Extended sampling step
$\varphi(t)$	Generating function/impulse response
$\Phi(t)$	Instantaneous phase

ω	Angular frequency
Ω	Maximum frequency of the spectrum obtained by Fourier transform
Ω_g	Maximum frequency of the spectrum obtained by Extended Fourier transform
$\sup_{n \in Z}(x_n)$	Smallest real number y that is greater than or equal to every number x_n, $n \in Z$

The topicality of the subject

Most of the digital design today is based on a synchronous approach – the total system is designed as the composition of one or more subsystems where each subsystem changes from one state to the next on the edges of a regular clock [25], [26]. By decreasing the size and increasing the speed of the chips, two main problems arise:

1) clock skew – the clock signal arrives at different components at different times – this can be caused by temperature variations, material imperfections and many other different things;
2) thermal problem – in a synchronous circuit many gates switch because they are connected to the clock, not because they have new inputs to process – this leads to an increase in energy dissipation and requires sophisticated heat removal technologies.

Consequently, as feature sizes reduce and chips encompass more functionality, the global clock is becoming increasingly inefficient [26].

These problems have renewed an interest in asynchronous design which in general uses no clock to govern the timing of state changes. Subsystems exchange information at mutually negotiated times with no external timing regulation [2], [9], [10], [19], [26]. This gives asynchronous circuits inherent properties that can be exploited to advantage in the areas listed below [28]:

1) low power consumption due to fine-grain clock gating and zero standby power consumption;
2) high operating speed (operating speed is determined by actual local latencies rather than global worst-case latency);
3) less emission of electro-magnetic noise due to the local clocks tend to tick at random points in time;
4) robustness towards variations in supply voltage, temperature, and fabrication process parameters;
5) better composability and modularity;
6) no clock distribution and clock skew problems.

Despite these advantages, the use of asynchronous systems in real life applications is not widespread due to the incompatibility with the classical (synchronous) systems. For example, in case of asynchronous systems asynchronous analog-to-digital converters (AADC) are used to transform analog signals to digital signals, and the samples obtained in this way are usually spaced non-uniformly [2], [15]. Such technique allows to create signal-dependent AADC, the power consumption of which depends on the signal being sampled [2], [13] – in high frequency regions more samples are obtained and more power is consumed, and in low frequency regions – less samples are obtained and less power is required for data acquisition. This allows reducing the total power consumption of the device and the number of obtained samples, which is of particular importance in wireless sensor networks [23], however, at the same time, this complicates the processing of obtained samples due to their irregular placement, so that the classical signal processing in this case is not applicable.

One of the ways to connect asynchronous systems with synchronous systems is to resample the signal from non-uniformly to uniformly spaced samples which equals to 1) recovery of the continuous signal and then – 2) uniform sampling of the reconstructed signal. The problem in this case is to develop the methods for recovery of the signals from their irregular samples.

The aim of the thesis

The aim of the thesis is to develop a theoretical justification for the assumption that the signals with time-varying spectral content can be accurately represented by samples obtained in signal-dependent way with more samples taken at high frequency regions and less samples – at low frequency regions, as well as to investigate how this knowledge can be used for recovery of the signals sampled in signal-dependent way.

The following objectives are set to fulfill the aim of the research:

- investigate different sampling methods found in literature;
- develop theory and methods for signal-dependent sampling and reconstruction.

Research methods

The research methods included the analytical derivations of the formulated theorems and developed methods, which was later experimentally verified by numerical simulations using MATLAB.

Scientific novelty and the main results

The scientific novelty of the thesis is associated with the developed theory and methods for signal-dependent sampling and reconstruction. The main results are:

- ✔ an extended Fourier series for analysis of signals with time-varying spectral content is proposed;
- ✔ an extended sampling theorem for signal-dependent sampling according to the maximum instantaneous frequency of the signal is proposed;
- ✔ different methods for estimation of the maximum instantaneous frequency of the signal are developed;
- ✔ a sufficient condition for perfect reconstruction of the signals from irregular samples is obtained, which allows the distances between consecutive samples to exceed the Nyquist step;
- ✔ several signal reconstruction methods from irregular samples are developed and verified by numerical simulations on different signals.
- ✔ a printed circuit board for level-crossing sampling is developed.

Theses to be defended

1. The obtained Extended Fourier series, which is composed of harmonics of time-varying frequencies, extends the set of those periodic functions that can be expressed by a finite number of components.
2. Those signals that have bandlimited spectra obtained by an extended Fourier transform can be completely represented by their samples, the time locations of which are determined by the frequency functions of the components of their spectra.
3. The sampling density that is needed for equally precise approximation of the signal in case of signal-dependent sampling, which considers the time-varying spectral content of the signal, can reduce in comparison to uniform sampling.
4. Those signals that have bandlimited spectra obtained by an extended Fourier transform can be perfectly reconstructed from their level-crossing samples even if the maximum distance between consecutive samples exceeds the Nyquist step.

Practical value

The theory and methods developed within this thesis can be used for signal-dependent sampling and processing with the aim to reduce the energy consumption of data acquisition devices, which is of particular importance in wireless sensor networks, as well as to improve the quality of reconstruction of signals sampled in signal-dependent way.

Approbation

The research results of the thesis were presented at the following conferences:

1. *The 2013 European Signal Processing Conference (EUSIPCO 2013), Marrakech, Marocco, September 9-13, 2013.
2. The 2012 European Signal Processing Conference (EUSIPCO 2012), Bucharest, Romania, August 27-31, 2012.
3. The 9th International Conference on Sampling Theory and Applications (SampTA 2011), Singapore, May 2-6, 2011.
4. The 2010 European Signal Processing Conference (EUSIPCO 2010), Aalborg, Denmark, August 23-27, 2010.
5. The 8th International Conference on Sampling Theory and Applications (SampTA 2009), Marseille, France, May 18-22, 2009.
6. International Conference on Signal Processing and Multimedia Applications (SIGMAP 2008), Porto, Portugal, July 26-29, 2008.
7. The 7th International Conference on Sampling Theory and Applications (SampTA 2007), Thessaloniki, Greece, June 1-5, 2007.
8. Workshop on Digital Alias-free Signal Processing (WDASP 2007), London, UK, April 17, 2017.

* Accepted for presentation and publication

The research results are published in the following papers:

I *Greitans M., Shavelis R. Extended fourier series for time-varying filtering and reconstruction from level-crossing samples// Proc. EUSIPCO 2013. - 2013, Marrakech, Marocco.

II Shavelis R., Greitans M. Signal Sampling According to Time-Varying Bandwidth// Proc.

EUSIPCO 2012. - 2012, Bucharest, Romania. - pp. 1164–1168.

III Ozols K., Greitans M., Shavelis R. EEG Data Acquisition System Based on Asynchronous Sigma-Delta Modulator// Proc. BEC 2012. - 2012, Tallinn, Estonia. - pp. 183–186.

IV Greitans M., Shavelis R., Fesquet L., Beyrouthy T. Combined peak and level-crossing sampling scheme// Proc. SampTA 2011. - 2011, Singapore. - published on CD.

V Beyrouthy T., Fesquet L., Greitans M., Shavelis R., Roland R. An asynchronous FIR filter architecture coupled to a level-crossing ADC// Proc. SampTA 2011. - 2011, Singapore. - published on CD.

VI Greitans M., Shavelis R. Reconstruction of sequences of arbitrary-shaped pulses from its low-pass or band-pass approximations using spectrum extrapolation// Proc. EUSIPCO 2010. - 2010, Aalborg, Denmark. - pp. 1607–1611.

VII Greitans M., Shavelis R. Signal-Dependent Sampling and Reconstruction Method of Signals With Time-Varying Bandwidth// Proc. SampTA 2009. - 2009, Marseille, France. - published on CD.

VIII Homjakovs I., Greitans M., Shavelis R. Real Time Acquisition of Wideband Signals Data Using Non-Uniform Sampling// Proc. EUROCON 2009. - 2009, Saint-Petersburg, Russia. - pp. 1158–1163.

IX Greitans M., Shavelis R. Signal-Dependent Techniques for Non-Stationary Signal Sampling and Reconstruction// Proc. EUSIPCO 2009. - 2009, Glasgow, Scotland. - pp. 2613–2617.

X Greitans M., Shavelis R. Signal-Dependent Analysis of Signals Sampled By Send-on-Delta Sampling Scheme// Proc. SIGMAP 2008. - 2008, Porto, Portugal. - pp. 125–130.

XI Greitans M., Shavelis R. Speech sampling by level-crossing and its reconstruction using spline-based filtering// Proc. IWSSIP 2007. - 2007, Maribor, Slovenia. - 292–295.

XII Greitans M., Shavelis R. Spline-based signal reconstruction algorithm from multiple level crossing samples// Proc. SampTA 2007. - 2007, Thessaloniki, Greece. - pp. 60–66.

XIII Shavelis R. Sampling and Waveform Reconstruction of Signals on The Basis of Minimax Approach// Proc. WDASP 2007. - 2007, London, UK. - pp. 57–61.

XIV Shavelis R. Signal Reconstruction from Multiple Level Crossings Using Asymmetric Constructing Functions// Electronics and Electrical Engineering. - 2007. - vol. 77(5). - pp. 57–60.

* Accepted for publication

The structure of the thesis

The doctoral thesis contains introduction, five chapters, conclusions, references, 8 appendices, 61 figures, 132 pages in total. A list of references consists of 108 sources.

Introduction motivates the research and formulates the research aim and tasks.

The first chapter discusses the classical sampling theory and an extension of the standard sampling paradigm for a representation of functions in the more general class of shift-invariant functions spaces. Also, several variations and other extensions of sampling theory are shown.

The second chapter discusses several advancements of the classical sampling theory which are based on the fact that many natural signals can be sparsely represented using only a small set of suitably selected basis. In the end of the chapter, time encoding of the analog signals is outlined.

The third chapter presents theory and methods of signal dependent sampling and reconstruction developed by the author in accordance with the aim of the thesis to find a theoretical justification for the assumption that the signals with time-varying spectral content can be accurately represented by samples obtained in signal-dependent way with more samples taken at high frequency regions and less samples – at low frequency regions, as well as to investigate how this knowledge can be used for recovery of the signals sampled in signal-dependent way.

The fourth chapter demonstrates the use of the developed theory in order to reconstruct the signals from level-crossing samples. A sufficient condition for perfect recovery is formulated, which allows the distances between consecutive samples to exceed the Nyquist step.

The fifth chapter describes the practical implementation of the level-crossing sampling.

Conclusions summarizes the main results of the thesis. In appendices several mathematical derivations and a simulated electronic circuit for level-crossing sampling are given.

1. CLASSICAL SIGNAL SAMPLING AND RECONSTRUCTION

In the first chapter the classical sampling theory is discussed.

The sampling theorem was introduced to information theory by Shannon [24]. The equivalent forms of the theorem were also introduced by Whittaker [30] and Kotel'nikov [11].

The Shannon sampling theorem: if a signal $s(t)$ contains no frequencies higher than F_{max}, it is completely determined by giving its ordinates at a series of points spaced $T=1/(2F_{max})$ seconds apart.

The reconstruction formula that complements the sampling theorem is

$$s(t)=\sum_{n=-\infty}^{\infty} s(nT)\,\mathrm{sinc}(\pi t/T-n\pi), \tag{1.1}$$

where

$$\mathrm{sinc}(t)=\sin(t)/t. \tag{1.2}$$

1.1. Sampling of non-bandlimited signals

Shannon's sampling theory is applicable whenever the input function is bandlimited. When this is not the case, the standard signal-processing practice is to apply a low-pass filter prior to sampling in order to suppress aliasing. Schematic representation of the standard three-step sampling paradigm with $T=1$ is shown in Fig. 1.1 [27].

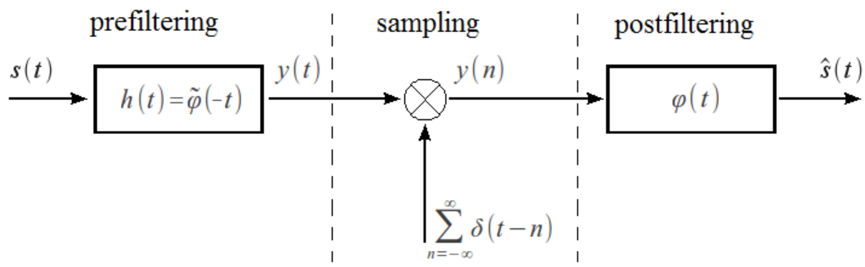

Fig. 1.1. Block diagram of sampling of non-bandlimited signals

The three steps are:

1) prefiltering – the analog input signal $s(t)$ is prefiltered with $h(t)$ to avoid aliasing;
2) sampling – the discrete signal $y(n)$ is obtained by sampling of $y(t)$;
3) postfiltering – the reconstructed output

$$\hat{s}(t)=\sum_{n=-\infty}^{\infty} y(n)\varphi(t-n) \tag{1.3}$$

is obtained by analog filtering of $y(n)$ with $\varphi(t)$.

In the traditional approach, the pre- and postfilters are both ideal low-pass: $h(t)=\varphi(t)=\mathrm{sinc}(\pi t)$ [27].

1.2. Extension of the Shannon's model

An approximation space $V(\varphi)$ is defined as

$$V(\varphi)=\left\{s(t)=\sum_{n=-\infty}^{\infty} c(n)\varphi(t-n)\right\}. \tag{1.4}$$

This means that any continuous function $s(t)\in V(\varphi)$ is characterized by a sequence of coefficients $c(n)$ that is the discrete signal representation that will be used to do signal processing calculations or to perform coding. These coefficients are not necessarily the samples of the signal, and $\varphi(t)$ can differ from $\mathrm{sinc}(\pi t)$ [27].

After defining the signal space $V(\varphi)$, the next task is to obtain the coefficients $c(n)$ in (1.4) such that the signal model is faithful approximation of some input signal $s(t)\in L_2$. The following three approaches are discussed [27]:

1) minimum error sampling;
2) consistent sampling;
3) interpolation.

After obtaining the coefficients $c(n)$, the approximation $\hat{s}(t)\in V(\varphi)$ of $s(t)\in L_2$ is found. As it follows from the error analysis [27], the best approximation is obtained in the case of minimum error sampling, and the least favorable approach due to aliasing is the sampling without analog prefiltering (interpolation).

1.3. Variations and extensions of sampling theory

There are different variations and extensions of sampling theory found in literature [8], for example, Kramer's generalized sampling theorem [12], Papoulis multichannel sampling [21], signal decomposition by wavelets [18], and irregular sampling [7], [14], [20], in the case of which the distances $\Delta t_n=t_{n+1}-t_n$ between consecutive samples are different.

2. ADVANCEMENTS OF THE CLASSICAL SAMPLING THEORY

In the second chapter several advancements of the classical sampling theory are discussed, which are based on the fact that many natural signals that occupy large bandwidth and thus require high sampling frequency can be compactly represented in an appropriate basis. The problem in this case is to find the methods of taking a small number of measurements that completely characterize the signal.

The first advancement is a digital alias-free signal processing (DASP) [4], which is a technique for overcoming the problems of aliasing at extended frequency ranges. Based on non-uniform or randomised sampling techniques and the development of novel algorithms, it creates the capacity to suppress potential aliasing crucial for high frequency applications and to reduce the complexity of designs.

The second advancement is a compressive sensing (CS) [5], which is a technique for acquiring a small number of measurements of the signal that has a sparse representation in some basis. CS computes the inner products of the signal and a randomized dictionary of test functions, and the signal is then recovered by a convex optimization that ensures the recovered signal is both consistent with the measurements and sparse.

The third advancement considers classes of signals with a finite rate of innovation (FROI) [29]. This technique allows to perfectly reconstruct the signals that are not bandlimited if they are sampled uniformly at or above the rate of innovation using an appropriate kernel.

The fourth approach (not related to the first three techniques) is a time encoding, which is a real-time, asynchronous mechanism for encoding the amplitude information of an analog bandlimited signal into a time sequence [15]. The advantage of time encoding is that it can be implemented in asynchronous analog circuits with low power consumption.

3. SIGNAL-DEPENDENT SAMPLING AND RECONSTRUCTION

The third chapter presents theory and methods of signal dependent sampling and reconstruction developed by the author. The main results are:

1) an extended Fourier series (EFS) for analysis of signals with time-varying spectral content is proposed;
2) an extended Fourier transform (EFT) (already defined in [17]) is obtained from EFS;
3) an extended sampling theorem considering the signals with bandlimited EFT spectra is proposed;
4) a connection between the classical and extended signal processing is shown by using the time-warped signal in Fig. 3.5;
5) a block diagram of signal-dependent analog-to-digital conversion considering the time-varying spectral content of the signal is shown;
6) an expression of the maximum instantaneous frequency of the signal, which is composed of harmonics of time-varying frequencies, is defined;
7) three methods for estimation of the maximum instantaneous frequency of the signal are proposed;
8) several examples of signal-dependent sampling and reconstruction are shown, and a comparison of the obtained results with the uniform sampling is given.

Next is a short description of the obtained results.

The majority of real life signals are non-stationary with time-varying frequency properties. The signal in this case is called non-stationary, if its spectral content at different time intervals is different (Fig. 3.1). On the contrary, the signal is called stationary, if its spectral content at different time intervals remains the same (Fig. 3.2).

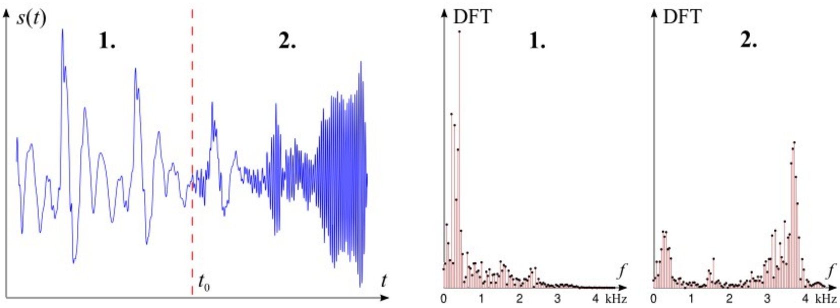

Fig. 3.1. Speech (non-stationary) signal and the magnitude of the DFT spectra of its two sub-intervals

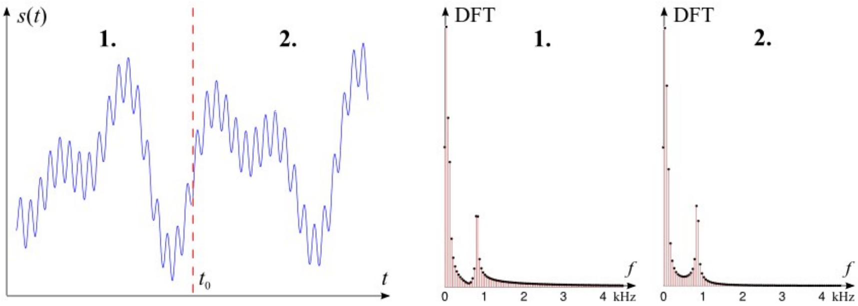

Fig. 3.2. Stationary signal and the magnitude of the DFT spectra of its two sub-intervals

As it follows from Fig. 3.1, the signal $s(t)$ at the first sub-interval up to t_0 varies slower than at the second sub-interval after t_0, and thus the question is: can the samples $s(t_n)$ at the first sub-interval be taken at less frequency than at the second sub-interval, and how to choose the sampling instants t_n for $s(t)$ to be reconstructable? These are the questions that are answered in the third chapter.

3.1. Extended Fourier series

As it follows from [I], periodic signals with period Θ can be expressed in an extended Fourier series (EFS) as

$$s(t)=\frac{1}{2}a_0+\sum_{n=1}^{\infty}a_n\cos\left(n\frac{2\pi}{\Phi(\Theta)}\Phi(t)\right)+b_n\sin\left(n\frac{2\pi}{\Phi(\Theta)}\Phi(t)\right), \tag{3.1}$$

where

$$\Phi(t)=\int_0^t\frac{1}{g(\tau)}d\tau, \tag{3.2}$$

and $g(t)>0$ is a periodic function with period Θ. The coefficients

$$a_n=\frac{2}{\Phi(\Theta)}\int_0^{\Theta}\frac{s(t)}{g(t)}\cos\left(n\frac{2\pi}{\Phi(\Theta)}\Phi(t)\right)dt \tag{3.3}$$

and

$$b_n=\frac{2}{\Phi(\Theta)}\int_0^{\Theta}\frac{s(t)}{g(t)}\sin\left(n\frac{2\pi}{\Phi(\Theta)}\Phi(t)\right)dt \tag{3.4}$$

are obtained, by minimizing the energy of the $1/\sqrt{g(t)}$-weighted error signal $(s(t)-y(t))/\sqrt{g(t)}$, where $y(t)$ denotes the right side signal of equation (3.1).

If instead of sines and cosines complex exponentials are used, then periodic signals are expressed in complex EFS as

$$s(t)=\sum_{n=-\infty}^{\infty} c_n e^{jn\frac{2\pi}{\Phi(\Theta)}\Phi(t)}, \tag{3.5}$$

where

$$c_n=\frac{1}{\Phi(\Theta)}\int_0^{\Theta}\frac{s(t)}{g(t)}e^{-jn\frac{2\pi}{\Phi(\Theta)}\Phi(t)}dt. \tag{3.6}$$

Bessel's inequality and Parseval's identity in this case are written as

$$\frac{1}{\Phi(\Theta)}\int_0^{\Theta}\frac{|s(t)|^2}{g(t)}dt \geq \sum_{n=-N}^{N}|c_n|^2 \tag{3.7}$$

and

$$\frac{1}{\Phi(\Theta)}\int_0^{\Theta}\frac{|s(t)|^2}{g(t)}dt = \sum_{n=-\infty}^{\infty}|c_n|^2. \tag{3.8}$$

Examples of EFS of two signals that are composed of 4 (on the left) and 7 (on the right) harmonics of frequencies $k f_1(t)$, $k=1,2,3,4$, and $m f_2(t)$, $m=1,2,\ldots,7$, are shown in Fig. 3.3. In the first case the function $g_1(t)=1/(2\pi f_1(t))$ is used for calculation of EFS, and in the second case – the function $g_2(t)=1/(2\pi f_2(t))$. If the signals are expressed in the classical Fourier series (FS) ($g_1(t)=g_2(t)=1$), then an infinite number of nonzero FS coefficients are obtained.

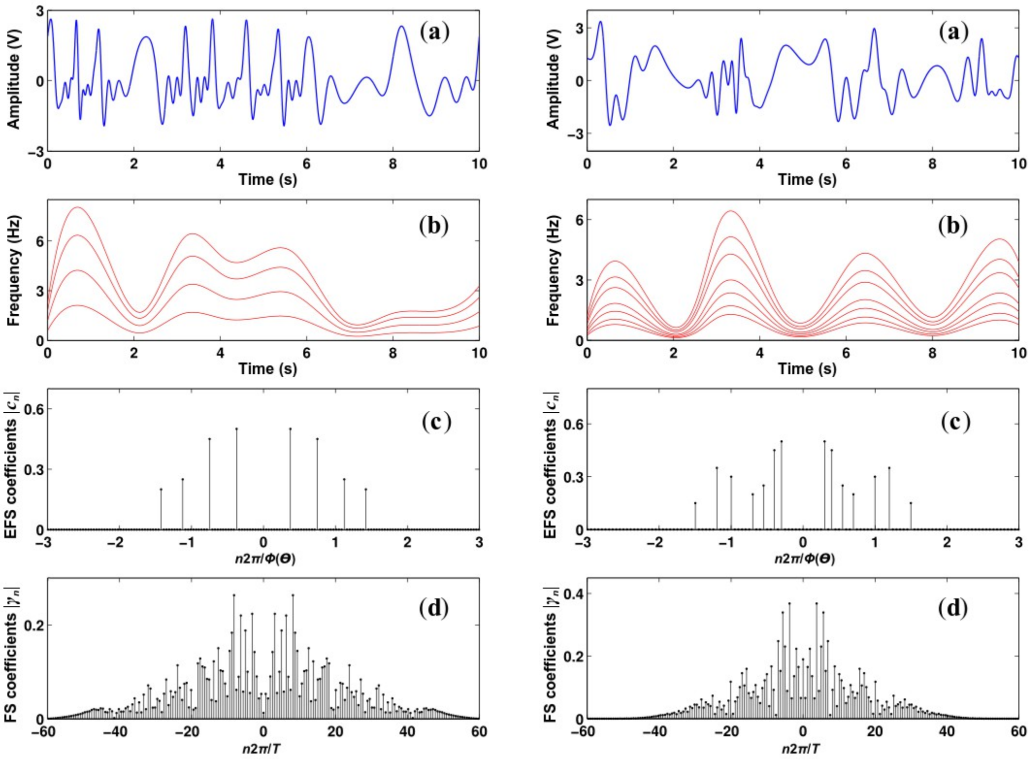

Fig. 3.3. EFS (c) un FS (d) amplitude spectra of periodic ($\Theta=10$ seconds) signals (a), that are composed of 4 (on the left) and 7 (on the right) harmonics of time-varying frequencies

As it follows from Fig. 3.3, non-bandlimited signal with time-varying spectral content can be compactly represented by EFS, if the appropriate function $g(t)$ depending on $s(t)$ is chosen.

3.2. Extended Fourier transform

If the period Θ and so the value $\Phi(\Theta)$ due to monotonic increase of $\Phi(t)$ tends to infinity, then from (3.6) follows:

$$S(\omega_g)=\lim_{\Theta\to\infty} c_n \Phi(\Theta)=\int_{-\infty}^{\infty} \frac{s(t)}{g(t)} e^{-j\omega_g \Phi(t)} dt, \tag{3.9}$$

which conforms to the definition of the extended Fourier transform (EFT) given in [17]:

$$S(\omega_g)=\tilde{F}[s(t), g(t)]=\int_{-\infty}^{\infty} \frac{s(t)}{g(t)} e^{-j\omega_g \Phi(t)} dt. \tag{3.10}$$

The inverse EFT (IEFT) [17]

$$s(t)=\tilde{F}^{-1}[S(\omega_g), g(t)]=\frac{1}{2\pi}\int_{-\infty}^{\infty} S(\omega_g) e^{j\omega_g \Phi(t)} d\omega_g, \tag{3.11}$$

follows from (3.5), when Θ tends to infinity:

$$s(t)=\lim_{\Theta\to\infty}\sum_{n=-\infty}^{\infty} \frac{1}{\Phi(\Theta)} S\left(n\frac{2\pi}{\Phi(\Theta)}\right) e^{jn\frac{2\pi}{\Phi(\Theta)}\Phi(t)}=\frac{1}{2\pi}\int_{-\infty}^{\infty} S(\omega_g) e^{j\omega_g \Phi(t)} d\omega_g. \tag{3.12}$$

If $g(t)=1$, then EFT and IEFT conform to the classical expressions of the direct and inverse Fourier transforms.

One example: EFT spectrum of the signal $x(t)=\cos(\psi(t))$, if $g(t)=1/\psi'(t)$, is:

$$\begin{aligned} X(\omega_g)=\tilde{F}[x(t), g(t)]=\int_{-\infty}^{\infty} \cos(\psi(t))\psi'(t) e^{-j\omega_g \psi(t)} dt=[u=\psi(t), du=\psi'(t)dt]= \\ =\int_{-\infty}^{\infty} \cos(u) e^{-j\omega_g u} du=\pi\delta(\omega_g-1)+\pi\delta(\omega_g+1). \end{aligned} \tag{3.13}$$

3.3. Extended sampling theorem

The extended sampling theorem follows from definitions of direct and inverse extended Fourier transforms in [II].

Extended sampling theorem: every bandlimited to $[-\Omega_g, \Omega_g]$ signal $s(t)$ with EFT spectrum $S(\omega_g)=\tilde{F}[s(t), g(t)]=0$, if $|\omega_g|>\Omega_g$, is completely determined by its samples $s(t_n)$ taken at instants $t_n=\Phi^{-1}(n\Upsilon)$ with a sampling step $\Upsilon\leq\pi/\Omega_g$.

The reconstruction formula is:

$$s(t) = \sum_{n=-\infty}^{\infty} s(t_n)\,\mathrm{sinc}\left(\frac{\pi}{\Upsilon}(\Phi(t) - \Phi(t_n))\right). \tag{3.14}$$

A sampling example of $s(t)$ at $t_n = \Phi^{-1}(n\,\Upsilon)$ depending on $\Phi(t)$ is shown in Fig. 3.4 – when function $\Phi(t)$ grows faster, more signal samples are obtained.

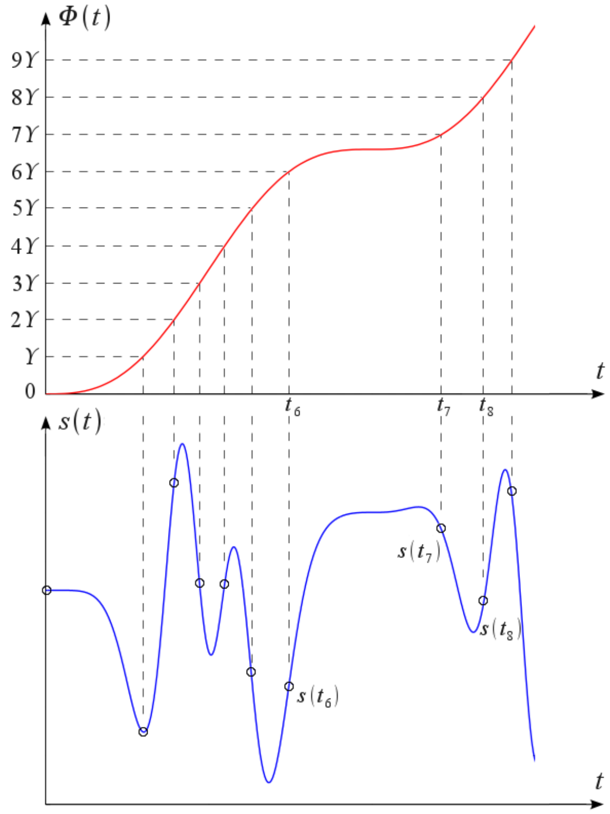

Fig. 3.4. Sampling of $s(t)$ according to $\Phi(t)$ – samples $s(t_n)$ are taken at $t_n = \Phi^{-1}(n\,\Upsilon)$

Example. EFT spectrum of the signal

$$x(t) = \sum_{n=-N}^{N} c_n e^{jn\frac{2\pi}{\Phi(\Theta)}\Phi(t)}, \tag{3.15}$$

if $g(t) = 1/\Phi'(t)$, is:

$$X(\omega_g) = \int_{-\infty}^{\infty} \frac{x(t)}{g(t)} e^{-j\omega_g \Phi(t)} dt = \sum_{n=-N}^{N} 2\pi\, c_n \delta\left(\omega_g - n\frac{2\pi}{\Phi(\Theta)}\right). \tag{3.16}$$

That means the signal is bandlimited to $\omega_g \in [-2\pi N/\Phi(\Theta), 2\pi N/\Phi(\Theta)]$, and is fully represented by samples $x(t_n)$ according to the expression

$$x(t) = \sum_{n=-\infty}^{\infty} x(t_n)\,\mathrm{sinc}\left(\frac{\pi}{\Upsilon}(\Phi(t) - \Phi(t_n))\right), \tag{3.17}$$

where $\Upsilon = \Phi(\Theta)/(2N)$ and $t_n = \Phi^{-1}(n\,\Upsilon)$.

3.4. Time-warped signals

The function $\Phi(t)$ that was previously defined by (3.2) can be used to transform the signal $s(t)$ into the time-warped signal $y(u)$ as shown in Fig. 3.5.

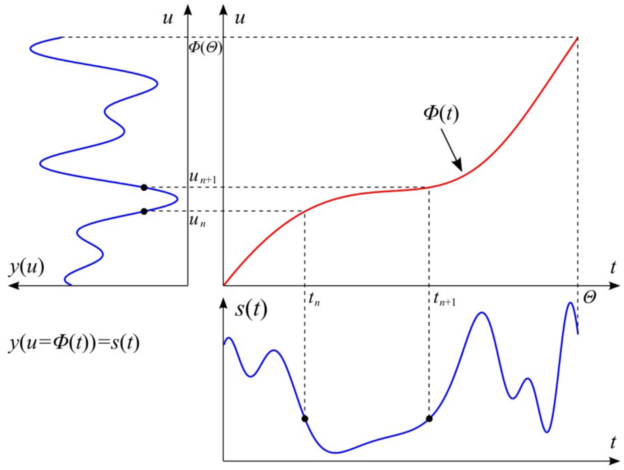

Fig. 3.5. The time-warped $u=\Phi(t)$ signal $y(u)$ obtained from $s(t)$: $y(\Phi(t))=s(t)$ and $y(u)=s(\Phi^{-1}(u))$

From Fig. 3.5 it can be concluded:

1) A finite length signal $y(u)$, $u\in[0,\Phi(\Theta)]$, can be expressed in the classical FS as

$$y(u)=\sum_{n=-\infty}^{\infty} c_n e^{jn\frac{2\pi}{\Phi(\Theta)}u}, \text{ where } c_n=\frac{1}{\Phi(\Theta)}\int_0^{\Phi(\Theta)} y(u)e^{-jn\frac{2\pi}{\Phi(\Theta)}u}du. \tag{3.18}$$

By putting $u=\Phi(t)$ and considering that $y(\Phi(t))=s(t)$ and $\Phi'(t)=1/g(t)$, from (3.18) the expressions of EFS (3.5) and (3.6) are obtained.

2) In similar way the expressions of EFT (3.10) and (3.11) follow from the classical Fourier transforms (FT) of $y(u)$:

$$\begin{aligned} Y(\eta)=F[y(u)]=\int_{-\infty}^{\infty} y(u)e^{-j\eta u}du=&\begin{bmatrix} u=\Phi(t),\ du=\Phi'(t)dt=(1/g(t))dt \\ y(\Phi(t))=s(t),\ \eta=\omega_g \end{bmatrix}= \\ =\int_{-\infty}^{\infty}\frac{s(t)}{g(t)}e^{-j\omega_g\Phi(t)}dt=\tilde{F}[s(t),g(t)]=S(\omega_g),& \end{aligned} \tag{3.19}$$

$$\begin{aligned} y(u)=F^{-1}[Y(\eta)]=\frac{1}{2\pi}\int_{-\infty}^{\infty} Y(\eta)e^{j\eta u}d\eta=&\begin{bmatrix} u=\Phi(t),\ t=\Phi^{-1}(u) \\ \eta=\omega_g,\ Y(\eta)=S(\omega_g),\ d\eta=d\omega_g \end{bmatrix}= \\ =\frac{1}{2\pi}\int_{-\infty}^{\infty} S(\omega_g)e^{j\omega_g\Phi(t)}d\omega_g=\tilde{F}^{-1}[S(\omega_g),g(t)]=s(\Phi^{-1}(u)).& \end{aligned} \tag{3.20}$$

Also, many EFT properties that correspond to the signal $s(t)$ can be obtained from FT properties of the time-warped signal $y(u)$.

3) If the FT spectrum of $y(u)$ is bandlimited: $Y(\eta)=0$, if $Y(\eta)>\Omega_g$, then $y(u)$ can be

represented by regular samples $y(n\Upsilon)$ according to the classical interpolation

$$y(u)=\sum_{n=-\infty}^{\infty} y(n\Upsilon)\operatorname{sinc}(\pi u/\Upsilon-n\pi), \tag{3.21}$$

where $\Upsilon\leq\pi/\Omega_g$. And again, by putting $u=\Phi(t)$ and considering that $y(\Phi(t))=s(t)$ and $\Phi'(t)=1/g(t)$, the extended sampling theorem (3.14) from (3.21) is obtained.

As it follows from the given three examples, the classical signal processing, which is applied to the time-warped signal $y(u)$, turns into the extended signal processing, which is applied to the original signal $s(t)$.

3.5. Sampling according to the time-varying spectral content of the signal

The real world signals are often non-stationary with time-varying frequency properties, which are estimated by various time-frequency analysis methods [1]. One of the most popular is the short-time Fourier transform (STFT), which calculates the FT spectra of the local sections $s(\tau)u(\tau-t)$ of the signal $s(\tau)$ at time instants t according to the expression

$$S(t,f)=\int_{t-\Theta/2}^{t+\Theta/2} s(\tau)u(\tau-t)e^{-j2\pi f\tau}d\tau, \tag{3.22}$$

where $u(\tau)$ is a window function which is nonzero for only a short period of time: $u(\tau)=0$, if $|\tau|>\Theta/2$. Given the non-stationary signal, the spectrum $S(t,f)$ at different t is different, and so is the bandwidth $f_{max}(t)$, which for some positive constant $d>0$ is estimated according to expressions: $|S(t,f)|\geq d$, if $|f|\leq f_{max}(t)$, and $|S(t,f)|<d$, if $|f|>f_{max}(t)$.

An example of the maximum instantaneous frequency $f_{max}(t)$, which is obtained from $S(t,f)$ of the speech signal, if $d=0.05$, is shown in Fig. 3.6.

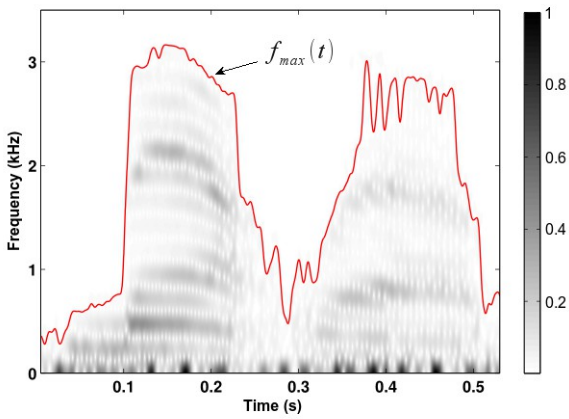

Fig. 3.6. Time-frequency distribution $S(t,f)$ of the speech signal and the estimated maximum instantaneous frequency $f_{max}(t)$

In order to take into account the function $f_{max}(t)$, which is called the maximum instantaneous frequency of the signal, for signal-dependent sampling according to the idea – more samples are taken at high frequency regions ($f_{max}(t)$ is large) and less samples at low frequency regions ($f_{max}(t)$is small), then considering the extended sampling theorem the samples of the signal are taken at $t_n = \Phi^{-1}(n\,\Upsilon)$, where

$$\Phi(t) = 2\pi \int_0^t f_{max}(\tau)\,d\tau = \int_0^t \omega_{max}(\tau)\,d\tau, \tag{3.23}$$

and Υ is the sampling step which is determined by the bandwidth of the EFT spectrum of the signal if $g(t) = 1/\omega_{max}(t)$. The block diagram of such sampling is shown in Fig. 3.7.

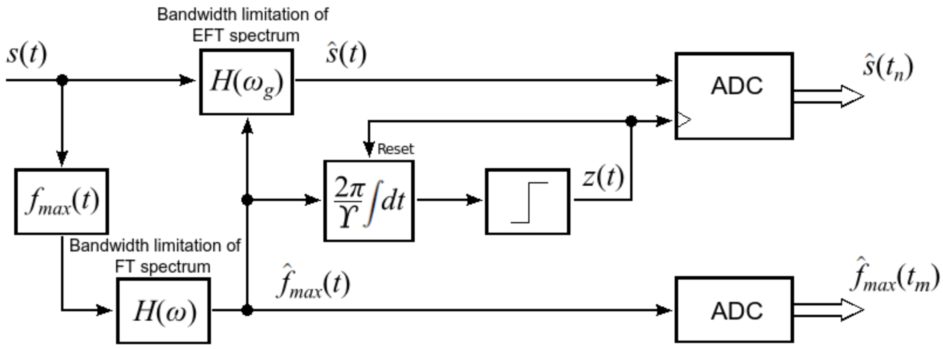

Fig. 3.7. Block diagram of signal-dependent analog-to-digital conversion considering the time-varying spectral content of the signal

In the figure the output of $f_{max}(t)$ is the maximum instantaneous frequency of $s(t)$, which is then filtered and used to limit the bandwidth of EFT spectrum of the input signal $s(t)$ to $\omega_g \in [-\Omega_g, \Omega_g]$. The filtered frequency function $\hat{f}_{max}(t)$ is also used for obtaining the time instants $t_n = \Phi^{-1}(n\,\Upsilon)$ in the following way. The output signal $\Phi(t)/\Upsilon$ of the integrator is connected to the input of the comparator, which compares this signal to the value of 1. At the time instant t_n, when $\Phi(t_n)/\Upsilon = 1$, the output binary signal $z(t)$ of the comparator changes its value from low to high level and after a short delay $\tau \ll t_{n+1} - t_n$ resets the output of the integrator to $\Phi(t_n + \tau)/\Upsilon = 0$, and then the signal $z(t)$ changes its value back to low level. In result the rising edges of $z(t)$ occur at the instants $t_n = \Phi^{-1}(n\,\Upsilon)$, and $z(t)$ is used to clock the upper ADC for capturing the signal samples $\hat{s}(t_n)$. At the same time the frequency function $\hat{f}_{max}(t)$ is sampled uniformly by the second ADC, since $\hat{f}_{max}(t)$ is needed for recovery of the signal $\hat{s}(t)$ according to the interpolation formula (3.14). This means that information about the analog input signal $\hat{s}(t)$ after its signal-dependent analog-to-digital conversion is carried by both the signal samples $\hat{s}(t_n)$, and the frequency samples $\hat{f}_{max}(t_m)$.

3.5.1. Estimation of the maximum instantaneous frequency of the signal

Given a signal

$$s(t)=\sum_{m=1}^{M} A_m \cos(\psi_m(t)) \tag{3.24}$$

with constant amplitudes A_m and time-varying frequencies $f_m(t)=\psi'_m(t)/(2\pi)>0$, the maximum instantaneous frequency $f_{max}(t)$ of $s(t)$ is defined as having values

$$f_{max}(\tau)=\max(f_1(\tau), f_2(\tau), \ldots, f_M(\tau)) \tag{3.25}$$

at any given $t=\tau$ [II]. An example of such a function of the signal which consists of $M=3$ cosines is shown in Fig. 3.8.

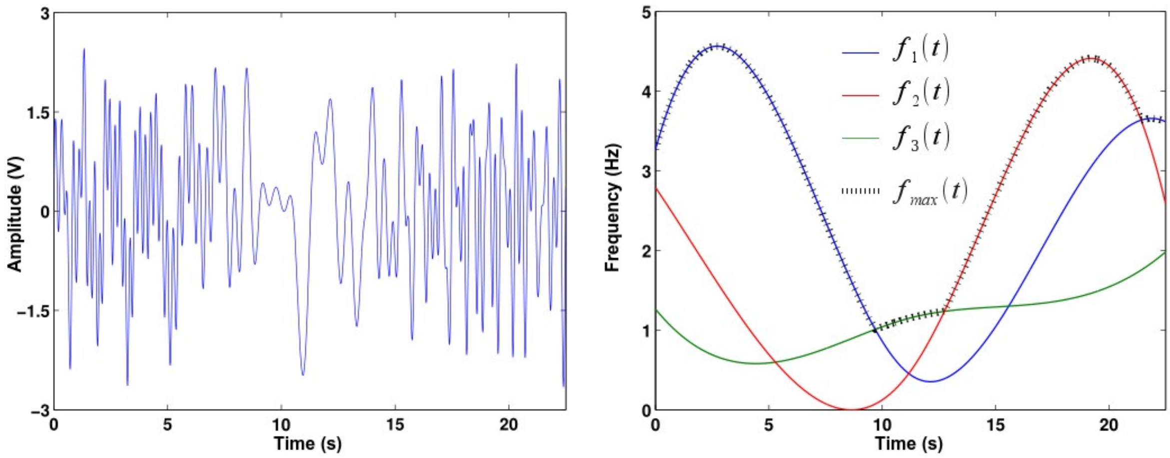

Fig. 3.8. The signal (on the left) and the frequency traces (on the right) of its $M=3$ cosines, and the maximum instantaneous frequency $f_{max}(t)$ of the signal

From the definition (3.25) follows, that the maximum instantaneous frequency $f_{max}(t)$ of the signal $x(t)=\sum_{m=1}^{M} A_m \cos(k_m \psi(t))$, where $k_1<\ldots<k_M$ are some positive coefficients, conforms to the instantaneous frequency of the highest component $A_M \cos(k_M \psi(t))$, and the EFT spectrum when $1/g(t)=k_M \psi'(t)$ is bandlimited to $\omega_g \in [-1, 1]$:

$$X(\omega_g)=\tilde{F}[x(t), g(t)]=\sum_{m=1}^{M} A_m \pi(\delta(\omega_g+k_m/k_M)+\delta(\omega_g-k_m/k_M)). \tag{3.26}$$

If no frequencies $f_m(t)$ of (3.24) are given or the signal differs from (3.24), then $f_{max}(t)$ can be estimated by using one of the three methods given in the full version of the thesis (the first method is based on the time-frequency analysis, the second method – on empirical mode decomposition (EMD) [II], and the third method – on local extrema of the signal).

3.5.2. Examples of signal-dependent sampling and reconstruction

Given the methods for estimation of $f_{max}(t)$, several comparisons of reconstruction quality depending on the number of samples that represent the signal in cases of uniform and signal-dependent sampling are given. One example is the speech signal (Fig. 3.9) that is taken from the TIMIT database (/timit/train/dr1/mtpf0/sx335.wav).

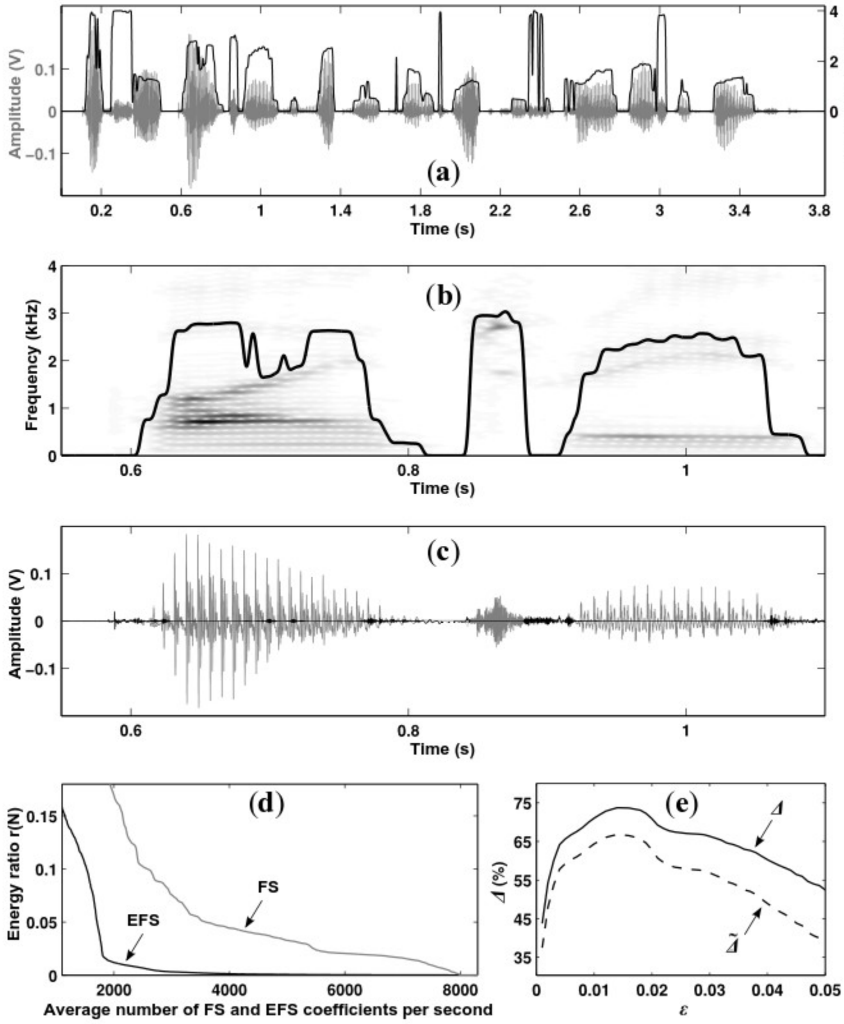

Fig. 3.9. Approximation of the speech signal $x(t)$ by EFS and FS: a) signal $x(t)$ and its maximum instantaneous frequency $\hat{f}_{max}(t)$ (black line), b) STFT of the signal fragment and the estimated frequency $\hat{f}_{max}(t)$ c) approximation $\hat{x}(t)$ (gray line) of $x(t)$ obtained by EFS and the error signal $x(t)-\hat{x}(t)$ (black line) at $\varepsilon=0.002$, d) the ratio $r(N)$ of the energies of the signals $x(t)-\hat{x}(t)$ and $x(t)$ depending on the average number of EFS and FS coefficients per second that are used to approximate the signal, e) reductions Δ and $\tilde{\Delta}$ in number of EFS coefficients (samples) that are needed to achieve the same precision ε of approximation as in the classical FS case

The maximum instantaneous frequency of the signal was estimated from its time-frequency distribution obtained by STFT using the Hamming window of length 20 ms. From the figure follows, that in the case of signal-dependent sampling less coefficients (samples) are needed to achieve equally precise approximation as in the classical uniform sampling. This is shown by (d) and (e) curves – (d) shows the energy ratio $r(N)$ of the error signal $x(t)-\hat{x}(t)$ and the original signal $x(t)$ depending on the number $2N+1$ of the terms that are used to approximate the signal, and (e) shows how many coefficients (samples) in the case of EFS are needed less than in the case of FS to obtain the same energy ratios $r(N_{EFS})=r(N_{FS})=\varepsilon$. The curve $\tilde{\Delta}$ corresponds to the case, when in addition to EFS coefficients the samples of the frequency function $\tilde{f}_{max}(t)$ that is bandlimited to $\omega\in[-500\pi, 500\pi]$ are taken into account.

4. LEVEL-CROSSING SAMPLING

The fourth chapter discusses the level-crossing (LC) sampling approach according to which the samples are taken whenever the analog signal crosses any of the previously set levels (Fig. 4.1) [2].

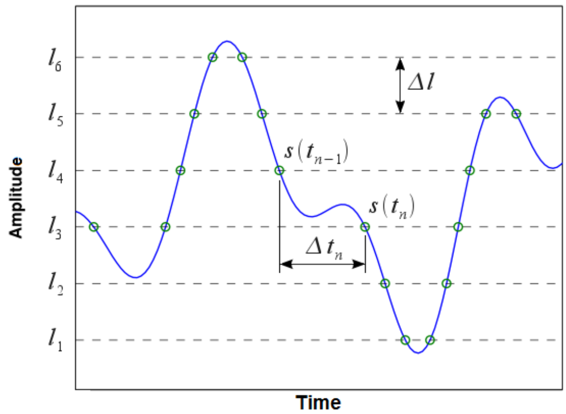

Fig. 4.1. Level-crossing sampling – the samples $s(t_n)$ are taken at the crossings of $s(t)$ with the levels $l_1, l_2, l_3, \ldots$

LC sampling gives signal samples that are spaced non-equidistantly with the distances $\Delta t_n = t_n - t_{n-1}$ being dependent on the locations of the levels and the maximum instantaneous frequency of the signal. Such approach allows to simplify the data acquisition, but complicates the processing of the obtained LC samples due to non-uniformity on the time axis. The samples can be processed either by asynchronous systems [22], [V], or by synchronous systems if only the discrete signal prior to processing is resampled from LC samples to uniform samples. In the second case the signal processing possibilities after resampling are larger and therefore the recovery of the signal from LC samples is the topic of the fourth chapter [VII], [IX], [X], [XI], [XII], [XIV]. The main results are as follows:

1) the method for estimation of the maximum instantaneous frequency from LC samples is proposed;
2) a sufficient condition for perfect reconstruction of the signals from irregular samples is obtained, which allows the distances between consecutive samples to exceed the Nyquist step, which is the classical limitation of the reconstruction methods found in literature [6], [7], [16];
3) several signal reconstruction methods from irregular LC samples are proposed, all of which can be realized in two ways: the first is to reconstruct the time-warped signal and then by its inversion to obtain the original signal (for time warping the estimated

maximum instantaneous frequency is used), or the second way is to directly reconstruct the original signal using the extended versions of the classical methods that are used in the first case for recovery of the time-warped signal;

4) the developed methods are verified by numerical simulations on various signals, and the obtained results allows to conclude that the application of signal-dependent theory in signal recovery from LC samples allows to improve the accuracy of reconstruction.

Sufficient condition for perfect recovery. In order to assure the proper signal reconstruction an appropriate sampling criterion should be respected during the sampling process [20]. As shown in [3], [8], [20], a bandlimited to $\omega \in [-\Omega, \Omega]$ signal can be reconstructed from its non-uniformly spaced samples if the average sampling frequency $\bar{f}_d > \Omega/\pi$, and therefore the sufficient condition for perfect recovery can be written as [6], [7], [16]:

$$\Delta t_{max} = \sup_{n \in N} (t_n - t_{n-1}) < \frac{\pi}{\Omega}. \tag{4.1}$$

In the case of LC sampling the fulfillment of (4.1) is hard to predict due to the distances $\Delta t_n = t_n - t_{n-1}$ between consecutive samples depend not only on the locations of the levels $l_1 < l_2 < \cdots < l_M$, but also on the signal itself. The more dense is the placement of l_m, the higher is the probability that the condition (4.1) fulfills, however, too many levels decrease the energy efficiency of the data acquisition due to an increased number of LC samples per second.

In order to avoid too high sampling densities, the sufficient condition (4.1) is written not for the signal $s(t)$, but for the time-warped signal $y(u)$ shown in Fig. 4.2. If the FT spectrum of $y(u)$ is bandlimited to $[-\Omega_g, \Omega_g]$, then the sufficient condition for perfect recovery of $y(u)$ from irregular samples $y(u_n)$ is:

$$\Delta u_{max} = \sup_{n \in N} (u_n - u_{n-1}) < \frac{\pi}{\Omega_g}. \tag{4.2}$$

By putting $u = \Phi(t)$ and considering that $y(\Phi(t)) = s(t)$ and $\Phi'(t) = 1/g(t)$, the equivalent condition for perfect recovery of the signal $s(t)$ from $s(t_n)$, if its EFT spectrum $S(\omega_g) = \tilde{F}[s(t), g(t)]$ is bandlimited to $\omega_g \in [-\Omega_g, \Omega_g]$, becomes [I]:

$$\sup_{n \in N} (\Phi(t_n) - \Phi(t_{n-1})) < \frac{\pi}{\Omega_g}. \tag{4.3}$$

By comparing (4.3) with (4.1), it can be concluded that the maximum distance Δt_{max}

between consecutive samples in the latter case can considerably exceed the Nyquist step π/Ω, and depends on the function $\Phi(t)$. One such example is shown in Fig. 4.2 – the large distance Δt_n between the LC samples $s(t_{n-1})$ and $s(t_n)$ by time warping $u=\Phi(t)$ transforms into a small distance Δu_n between the same LC samples $y(u_{n-1})=s(t_{n-1})$ and $y(u_n)=s(t_n)$ of the time-warped signal $y(u)$.

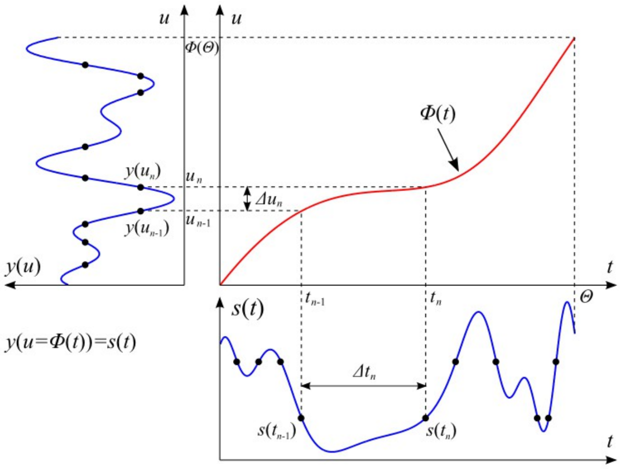

Fig. 4.2. Transformation of the large distance Δt_n into the small distance Δu_n by time warping $u=\Phi(t)$

The methods for estimation of the function $\Phi(t)$ from LC samples, as well as for recovery of the signals are given in the full version of the thesis.

5. PRACTICAL IMPLEMENTATION OF LC SAMPLING

In the fifth chapter the practical implementation of LC sampling is described. In order to reduce the sensitivity to noise and to avoid too small distances between the samples which can cause errors in the conversion, then every next LC sample is taken only when the difference between the signal and its previous sample reaches the threshold Δl (Fig. 5.1).

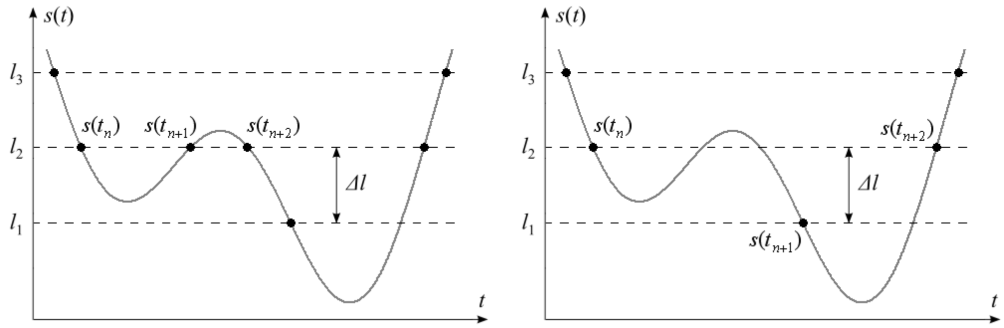

Fig. 5.1. Level-crossing (on the left) and send-on-delta (on the right) sampling

Such send-on-delta sampling can be realized according to the following principle (Fig. 5.2). The input signal $s(t)$, if $t<t_1$, is located between two levels: $y_{down}(t)=l_4$ and $y_{up}(t)=l_4+2\Delta l=l_6$. When the signal decreases and crosses the lower level l_4 at t_1, then the values of $y_{down}(t)$ and $y_{up}(t)$ are increased by Δl, and the signal $s(t)$, if $t_1 \le t < t_2$, is located between the new levels $y_{down}(t)=l_3$ and $y_{up}(t)=l_3+2\Delta l=l_5$. In the same way the values of $y_{down}(t)$ and $y_{up}(t)$ are decreased at t_2 and t_3, and the signal $s(t)$, if $t_3 \le t < t_4$, is located between the levels $y_{down}(t)=l_1$ and $y_{up}(t)=l_1+2\Delta l=l_3$. In turn, when the signal increases and crosses the upper levels l_3 and l_4 at t_4 and t_5, the values of $y_{down}(t)$ and $y_{up}(t)$ are increased by Δl. In result, the signal $s(t)$ is almost always located between the levels $y_{down}(t)$ and $y_{up}(t)$, the crossings of which are recorded as the LC samples of $s(t)$.

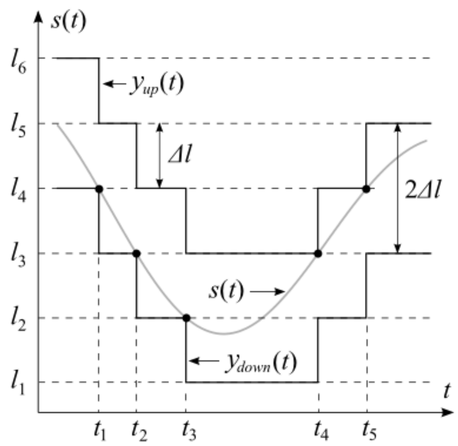

Fig. 5.2. The illustration of the principle of the practical realization of send-on-delta sampling

Such send-on-delta sampling principle can be implemented according to the block diagram shown in Fig. 5.3.

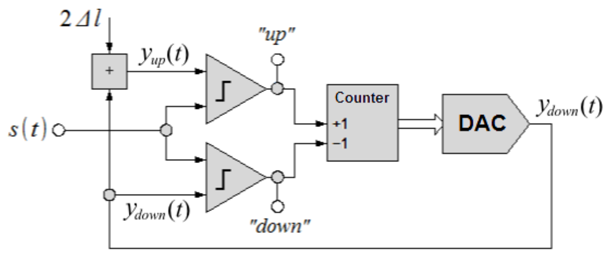

Fig. 5.3. Block diagram of the practical implementation of send-on-delta sampling

The input signal $y_{down}(t)<s(t)<y_{up}(t)$ is compared to the levels $y_{down}(t)$ and $y_{up}(t)=y_{down}(t)+2\Delta l$ by the two comparators. If the signal $s(t)$ increases and crosses the upper level $y_{up}(t)$, then a short pulse "up" is generated by the first comparator and the output of the DAC $y_{down}(t)$ increases by Δl. If the signal $s(t)$ decreases and crosses the lower level $y_{down}(t)$, then a short pulse "down" is generated by the second comparator and the output of the DAC decreases by Δl. This ensures the inequation $y_{down}(t)<s(t)<y_{up}(t)$ holds almost all the time.

An electronic scheme that corresponds to the block diagram shown in Fig. 5.3 is included in the eighth appendix of the thesis. According to the scheme the printed circuit board that performs LC sampling using 16 uniformly distributed levels from -10V to +10V was produced. From the measurements if follows, that the maximum frequency of the signal that can be sampled is 10 kHz. In the case of higher frequencies the levels $y_{up}(t)$ and $y_{down}(t)$ are not capable of following the rapid changes in the input signal. One example of the speech signal send-on-delta sampling that was captured by an oscilloscope is shown in Fig. 5.4.

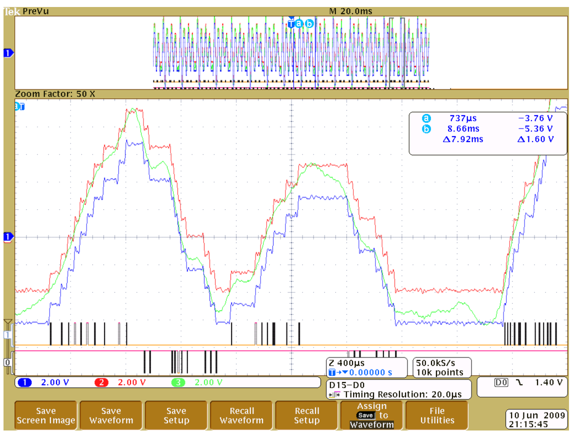

Fig. 5.4. Send-on-delta sampling of the speech signal (green line): blue line signal $y_{down}(t)$ corresponds to the output of the DAC, red line signal – to the raised by $2\Delta l$ signal $y_{up}(t)$, and the black line signals (at the bottom) are the outputs "up" and "down" of the comparators

Conclusions

The aim of the thesis was to develop a theoretical justification for the assumption that the signals with time-varying spectral content can be accurately represented by samples obtained in signal-dependent way with more samples taken at high frequency regions and less samples – at low frequency regions, as well as to investigate how this knowledge can be used for recovery of the signals sampled in signal-dependent way.

In accordance with the set objective of developing theory and methods for signal-dependent sampling and reconstruction, the author has obtained the following main results:

1. The extended Fourier series consisting of sines and cosines of time-varying frequencies is proposed which allows to reduce the number of coefficients that are needed to represent the signals with time-varying spectral content (this is demonstrated in section 3.5.2).
2. The extended sampling theorem for signal sampling according to the monotonically increasing function $\Phi(t)$ is proposed.
3. Several methods for estimation of the maximum instantaneous frequency $\hat{f}_{max}(t)$ of the signal are proposed – this frequency is used for signal-dependent sampling according to the extended sampling theorem: from $\hat{f}_{max}(t)$ follows $\Phi(t)$, and from $\Phi(t)$ – the sampling instants $t_n = \Phi^{-1}(n\,\Upsilon)$. This answers to the first question of how to choose the sampling instants depending on the time-varying spectral content of the signal.
4. By considering the extended sampling theorem, the sufficient condition (4.3) for perfect reconstruction of the signals from irregular samples is obtained, which allows the distances between consecutive samples to exceed the Nyquist step. This answers to the second question of how the developed theory can be used for recovery of the signals sampled in signal-dependent way.
5. In accordance with the sufficient condition (4.3), several signal reconstruction methods from irregular LC samples are proposed, one of which exploits the knowledge of signal locations between the consecutive LC samples.
6. The developed methods are verified by numerical simulations on various signals, and the evaluation of the obtained results and conclusions are given.
7. The printed circuit board that performs the signal-dependent sampling based on level-crossing concept is developed.

From the given results it can be concluded, that the aim of the thesis is achieved.

Bibliography

1. *Allen R.L., Mills D.W. Signal Analysis: Time, Frequency, Scale, and Structure. - Wiley, 2004. - p. 966.*
2. *Allier E., Sicard G., Fesquet L. A New Class of Asynchronous A/D Converters Based on Time Quantization// Proc. Ninth International Symposium on Asynchronous Circuits and Systems. - 2003. - pp. 196–205.*
3. *Beutler F.J. Error Free Recovery from Irregularly Spaced Samples// SIAM Review. - 1966. - vol. 8(3). - pp. 328–335.*
4. *Bilinskis I. Digital Alias-free Signal Processing. - UK: Wiley, 2007. - 454 p.*
5. *Donoho D. Compressed sensing// IEEE Trans. Inform. Theory. - 2006. - vol. 52(4). - pp. 1289–1306.*
6. *Feichtinger H.G., Gröchening K. Theory and practice of irregular sampling// Benedetto J.J, Frazier M.W. Wavelets: Mathematics and Applications. - Boca Raton: CRC Press, 1994. - pp. 305–363.*
7. *Gröchenig K. Reconstruction algorithms in irregular sampling// Math. Comp. - 1992. - vol. 59(199). - pp. 181–194.*
8. *Jerri A.J. The Shannon sampling theorem – Its various extensions and applications: A tutorial review// Proc. IEEE. - 1977. - vol. 65. - pp. 1565–1596.*
9. *Kinniment D.J., Gao B., Yakovlev A.V., Xia F. Towards asynchronous A-D conversion// Proc. Fourth International Symposium on Advanced Research in Asynchronous Circuits and Systems. - 1998. - pp. 206–215.*
10. *Kinniment D.J., Yakovlev A.V., Gao B. Synchronous and asynchronous A-D conversion// IEEE Trans. on Very Large Integration Systems. - 2000. - vol. 8(2). - pp. 217–220.*
11. *Kotel'nikov V. A. On the transmission capacity of "ether" and wire in electrocommunications// Izd. Red. Upr. Svyazzi RKKA (Moscow). - 1933.*
12. *Kramer H.P. A generalized sampling theorem// J. Math. Phys. - 1959. - vol. 38. - pp. 68–72.*
13. *Kurchuk M., Tsividis Y. Digital Signal Processing in Continuous Time. - CMOSET 2010 Circuits Track Presentation Slides: CMOS Emerging Techologies, 2010.*
14. *Landau H.J. Necessary density conditions for sampling and interpolation of certain entire functions// Acta Math. - 1967. - vol. 117. - pp. 37–52.*
15. *Lazar A.A., Simonyi E.K., Tóth L.T. Time Encoding of Bandlimited Signals, an Overview//*

Proc. ICTSM 2005. - 2005, Dallas, USA.

16. *Lazar A.A., Tóth L.T. Perfect recovery and sensitivity analysis of time encoded bandlimited signals// IEEE Trans. Circuits and Systems-I: Regular Papers. - 2004. - vol. 51(10). - pp. 2060–2073.*
17. *Lee H., Bien Z. Linear Time-Varying Filter with Variable Bandwidth// Proc. ISCAS 2006. - 2006, Kos, Greece.*
18. *Mallat S. A theory of multiresolution signal decomposition: The wavelet representation// IEEE Trans. Pattern Anal. Machine Intell. - 1989. - vol. 11. - pp. 674–693.*
19. *Martin A.J., Nystrom M., Wong C.G. Three generations of asynchronous micro-processors// IEEE Design and Test of Computers. - 2003. - vol. 20(6). - pp. 9–17.*
20. *Marvasti F. Nonuniform Sampling Theory and Practice. - New York: Kluwer academic/Plenum Publishers, 2001. - 924 p.*
21. *Papoulis A. Generalized sampling expansion// IEEE Trans. Circuits Syst. - 1977. - vol. 24. - pp. 652–654.*
22. *Qaisar. S.M. Signal Driven Sampling and Processing: A Promising Approach for Computationally Efficient Adaptive Rate Solutions// PhD thesis . - Grenoble INP, Laboratory TIMA, Group CIS. - 2009. - 233. p.*
23. *Raghavendra C.S., Sivalingam K.M., Znati T.F. Wireless sensor networks. - New York: Springer, 2004. - 426 p.*
24. *Shannon C.E. Communication in the presence of noise// Proc. of the IRE. - 1949. - vol. 37(1). - pp. 10–21.*
25. *Smith S.C., Di J. Designing asynchronous circuits using NULL convention logic (NCL). - Morgan & Claypool Publishers, 2009. - 86 p.*
26. *Sparsø J., Furber S. Principles of Asynchronous Circuit Design - A Systems Perspective. - Boston: Kluwer Academic Publishers, 2001. - 360 p.*
27. *Unser M. Sampling – 50 years after Shannon// Proc. of the IEEE. - 2000. - vol. 88(4). - pp. 569–587.*
28. *Van Berkel C.H., Josephs M.B., Nowick S.M. Scanning the technology: Applications of asynchronous circuits// Proc. IEEE. - 1999. - vol. 87(2). - pp. 223–233.*
29. *Vetterli M., Marziliano P., Blu T. Sampling signals with finite rate of innovation// IEEE Trans. Sign. Proc. - 2002. - vol. 50. - pp. 1417–1428.*
30. *Whittaker J. M. The Fourier theory of the cardinal functions// Proc. Math. Soc. Edinburgh. - 1929. - vol. 1. - pp. 169–176.*